# Electronic Supplementary Information

**From gaseous HCN to nucleobases at cosmic silicate dust surface:**

**an experimental insight into the onset of prebiotic chemistry in space**

Rosangela Santalucia,[ab] Marco Pazzi,[a] Francesca Bonino,[ab] Matteo Signorile,[ab] Domenica

Scarano,[ab] Piero Ugliengo,[* ab] Giuseppe Spoto,[* ab] and Lorenzo Mino[ab]

[a] Department of Chemistry, University of Turin, 10125, Turin, Italy

[b] Nanostructured Interfaces and Surfaces (NIS) Interdepartmental Centre, 10125, Turin, Italy

Corresponding authors:

*Piero Ugliengo, Giuseppe Spoto

**Email:** piero.ugliengo@unito.it, giuseppe.spoto@unito.it

**Materials and Methods**

**Materials**

Four different synthetic materials were used as laboratory models for study the catalytic role of mineral surfaces in the HCN polymerization process:

i. **Amorphous silica, $SiO_2$ (Aerosil OX 50)**: commercial pyrogenic silica by Evonik, formerly Degussa (specific surface area 50 $m^2$/g). Before HCN adsorption, the sample was outgassed at 973 K to obtain a complete surface dehydration.

ii. **Amorphous magnesium silicate, $Mg_2SiO_4$ (AMS)**: prepared by Yamamoto et al. (28) via evaporation of the precursors, $Mg(OH)_2$ and $SiO_2$, in a high temperature plasma ($\sim$10,000 K) and following quenching (specific surface area $\approx$ 37 $m^2$/g).[1]

iii. **Crystalline magnesium silicate, $Mg_2SiO_4$ (CMS or Forsterite)**: prepared by heating the pristine AMS at 1073 K for 24 h in air. The specific surface area was of $\approx$ 26 $m^2$/g.[1] The complete surface dehydration of the magnesium silicate samples (AMS and CMS), prior the HCN adsorption, is attained by outgassing at 673 K.

iv. **Magnesium oxide, MgO**: prepared by thermal decomposition of $Mg(OH)_2$ in vacuo up to 1073 K. The specific surface area was $\sim$200 $m^2$/g.[2]

**Methods**

**Synthesis of HCN gas**. We have developed a safe and efficient procedure to produce HCN, alternative to the classical ones (typically the addition of acids to cyanide salts of alkali metals). It consists of (i) the reduction at 523 K of AuCN or AgCN (very stable cyanides safe to be handled without any special precaution) in $H_2$ atmosphere and in presence of small Pd particles as catalyst, (ii) the separation of HCN from other gaseous products by repeated freeze-thaw cycles and (iii) the further purification of HCN just before its dosage (by means of a vacuum line) on the solid of interest by flowing the gas over a desiccant ($CaCl_2$). Such method allows us to obtain HCN gas with high purity (without any trace of water and other contaminants).

***In situ* IR spectroscopy investigation**. For IR spectroscopic measurements all the powder samples were pressed in form of self-supporting pellets suitable for transmission IR measurements by means of all quartz IR cells equipped with IR transparent KBr windows. These cells allow the thermal pretreatments of the samples at high temperature (up to *ca*. 1073 K) under vacuo (final pressure $10^{-5}$ mbar) to remove all the surface adsorbed impurities as well as low temperature measurements (down to 100 K using liquid nitrogen as cooler). In typical experiments HCN was dosed from the gas phase (by means of a vacuum line permanently connected to the IR cell) on the samples kept at low temperature (estimated at *ca.* 150 K); the temperature was then allowed to freely rise up to 300 K while collecting spectral series at constant time intervals. The IR spectra were

collected on a Bruker EQUINOX 55 FTIR spectrometer, equipped with a DTGS detector, at a resolution of 2 cm$^{-1}$, by accumulating 128 scans to attain a good signal-to-noise ratio.

**Extraction of surface products and HR-MS analysis of the soluble fraction**. At the end of the IR spectroscopic measurements, the samples were removed from the cell, manually ground, and suspended in 1 mL of methanol. The suspension was sonicated for 30 min and then centrifuged for 10 min at 10000 rpm. The supernatant was removed and analyzed by direct infusion high-resolution mass spectrometry. HR-MS analyses of the washing solutions were performed using an LTQ Orbitrap mass spectrometer (Thermo Scientific) equipped with an electrospray ionization (ESI) source in negative ion mode. The source voltage was set to 4.48 kV. The heated capillary temperature was maintained at 270 K. Mass accuracy of recorded ions (vs calculated) was ± 1 mmu (without internal calibration). Samples were delivered directly to the mass spectrometer via a Hamilton microliter syringe at constant flow (10 μL/min). Data acquisition and processing were performed using the Xcalibur software (version 3.1.66.10; Thermo Fisher Scientific, San Jose, CA, USA). Elemental formula assignments were made by comparison of the observed m/z with calculated elemental formulas using H, C, N and O. We assumed that the elemental formula whose calculated m/z was closest to the observed m/z was the correct formula.

**Crystal structure of amorphous and crystalline Mg₂SiO₄ (AMS and CMS)**
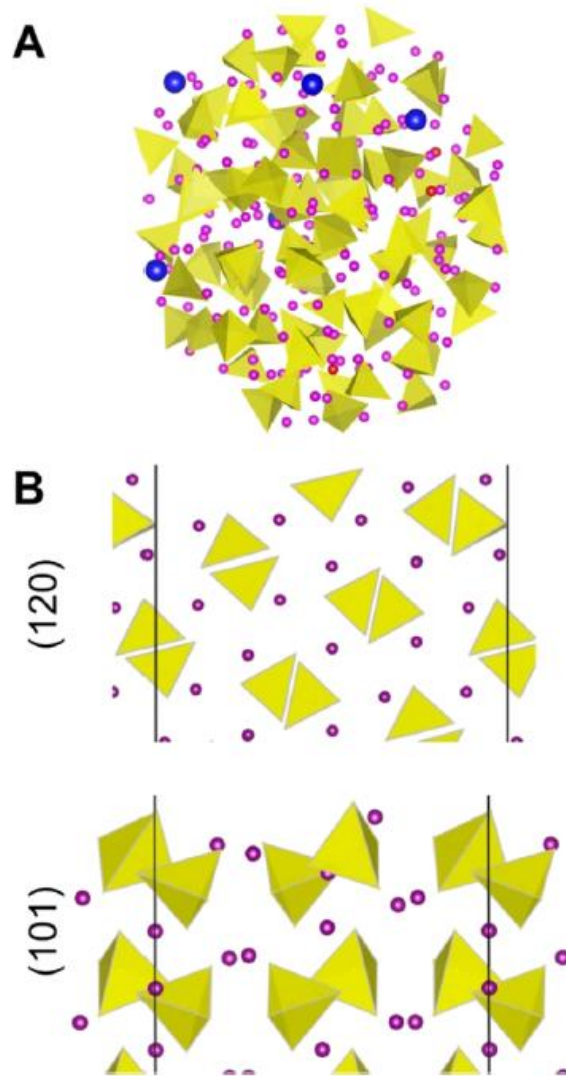


**Fig. S1**. (A) Computer generated structure of amorphous $Mg_2SiO_4$ nanograin as a model of interstellar core. (B) View along the [100] direction of the (120) and (101) crystalline forsterite surfaces. The unit cell borders are reported by thin black lines. Color code: Mg in purple; $SiO_4$ tetrahedra in yellow; O not belonging to $SiO_4$ units in blue. Reproduced with permission from Ref.[1]

**HR-MS spectra of amorphous and crystalline Mg₂SiO₄ samples (AMS and CMS)**

The HRMS spectra of the soluble fractions extracted from the AMS and CMS (forsterite) samples after HCN dosage are show in **Fig. S2**. The same species present for the MgO sample with different relative intensity were observed. Contrary to MgO sample, the most intense peak is the mass at m/z 107 corresponding to the tetramer of HCN (DAMN). The other masses are present in minor amount. This means that, in accordance with the IR data, investigated silicates show a lower reactivity toward the hydrogen cyanide. The surface sites are able to promote the initial oligomerization of HCN until the formation of the tetramer. Furthermore, the mass at m/z 132 is the second peak most intense in the AMS spectrum. This confirms that the favored pathway is those that lead to the 5-amino-1H-imidazole-2,4-dicarbonitrile (m/z 132). The silicates AMS and CMS, in addition to having a lower specific surface area respect than MgO sample, are characterized by a minor amount both of Lewis basic sites and defectives sites. That would explain the lower reactivity of such materials.
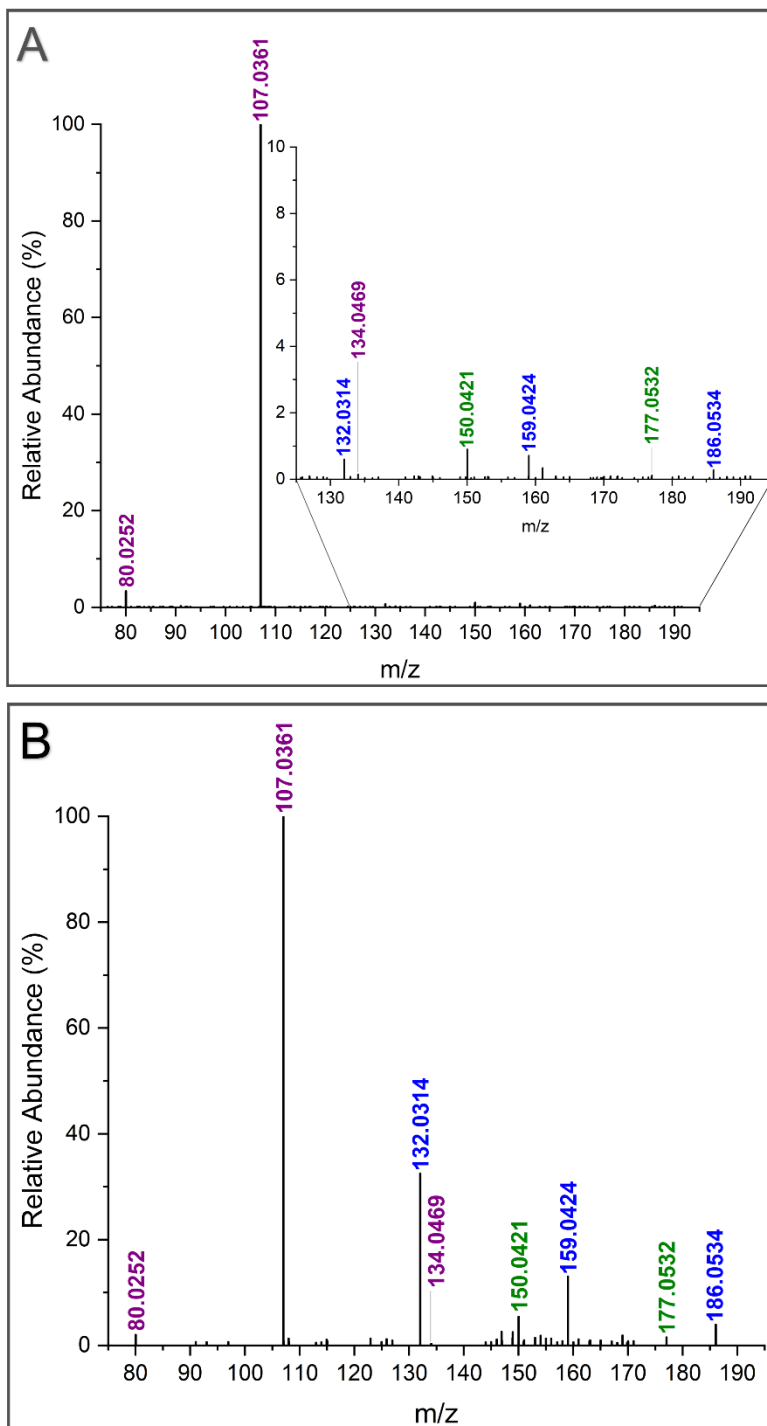
**Fig. S2.** Direct infusion ESI-HRMS spectra (acquired in negative ion mode) of the solutions resulting from extraction (using methanol) of the reaction products formed after HCN gas adsorption on CMS (panel A) and AMS (panel B) samples. The peaks of interest are indicated by their m/z values. More details are shown in **Table 1** in the main text.

**MS/MS fragmentation spectra of reaction products.**

Further confirmation of the identified products comes from the ESI-MS/MS direct infusion data which allowed us to isolate and fragment each mass of interest. The obtained products ions are summarized in **Table S1**, while the $MS^2$ spectra with related fragments structures are reported in **Fig. S3**. The fragmentation profiles indicate that the species are closely related to each other. The fragmentation profiles ($MS^2$) reveal that the selected species mainly dissociate by the loss of HCN (-27) or its dimer, iminoacetonitrile ($H_2C_2N_2$, -54). In addition, fragments by loss of cyanogen ($C_2N_2$, -52), carbodiimide (HNCNH, -42) and/or cyanamide ($NH_2CN$, -42), DAMN ($H_4C_4N_4$, -108), methylamine ($CH_3NH_2$, -31), and methyleneimine ($H_2CNH$, -29) have been found. About the dissociation of oxygenated species (m/z 150 and 177) losses of water ($H_2O$, -18) or isocyanic acid (HNCO, -43) have been detected. The agreement between our fragmentation pattern of the mass m/z 134 and that reported in literature[3] represents a further prove of the presence of adenine in our mixtures.

**Table S1.** Collision-induced dissociation MS/MS data of main ions identified for all samples (see **Fig. 3** of the main text and **Fig. S2**). The related fragmentation spectra (MS/MS) are shown in **Fig. S3**.

| Compound | Chemical Formula | Precursor ion m/z | Product ions m/z[a] | CID-MS$^2$ (eV) |
|---|---|---|---|---|
| A | $[C_5H_4N_5]^-$ | 134.0469 | 107.0360 92.0251 80.0251* | 35 |
| B | $[C_5H_2N_5]^-$ | 132.0313 | 117.0041 105.0204* 78.0095 | 30 |
| C | $[C_6H_3N_6]^-$ | 159.0424 | 132.0310* 107.0357 80.0249 | 30 |
| D | $[C_7H_4N_7]^-$ | 186.0534 | 159.0419* 132.0310 | 25 |
| E | $[C_5H_4ON_5]^-$ | 150.0421 | 132.0313 123.0310* 107.0360 80.0251 | 30 |
| F | $[C_6H_5ON_6]^-$ | 177.0532 | 134.0469* | 25 |
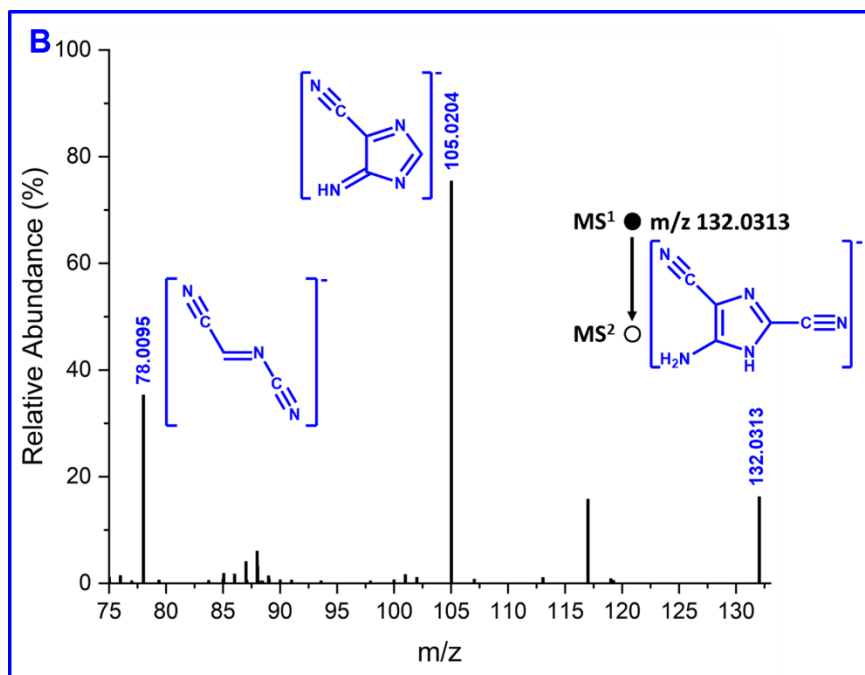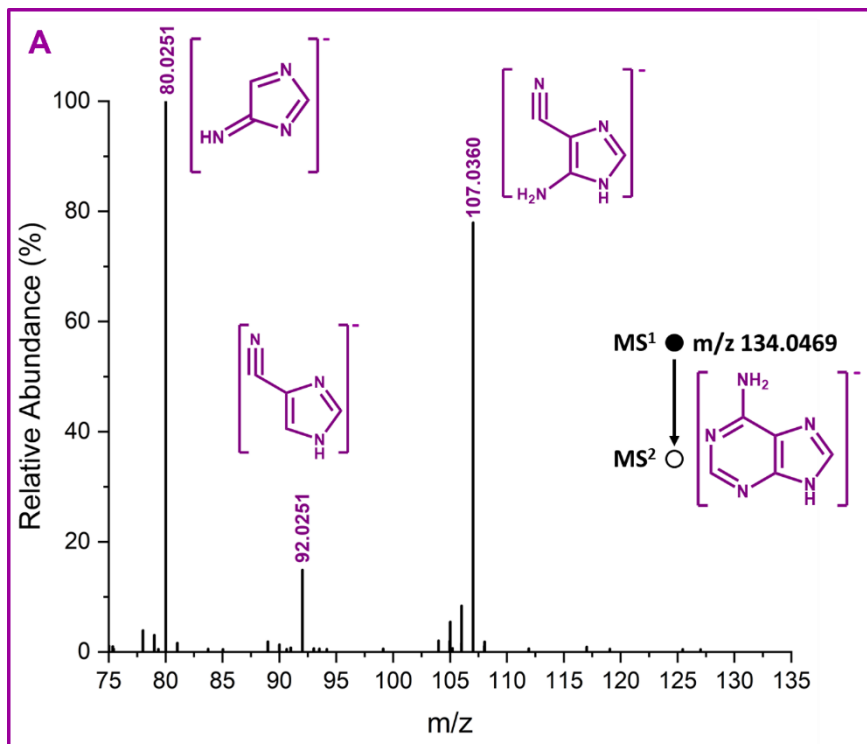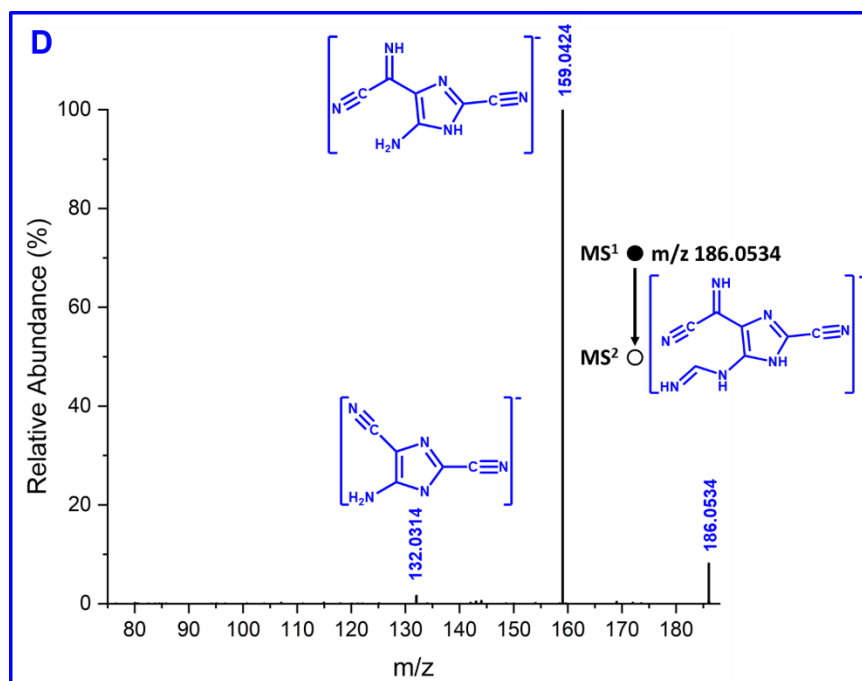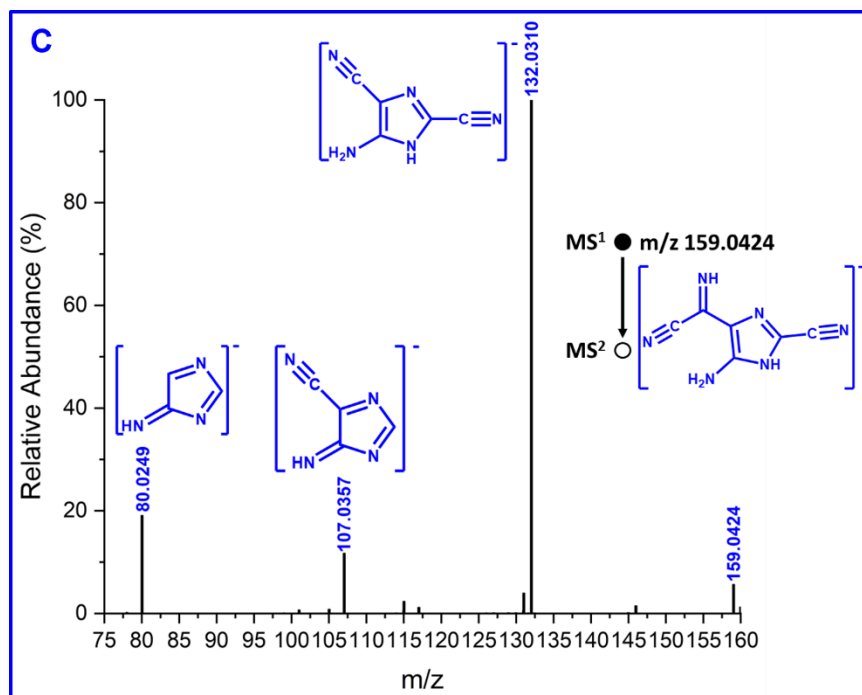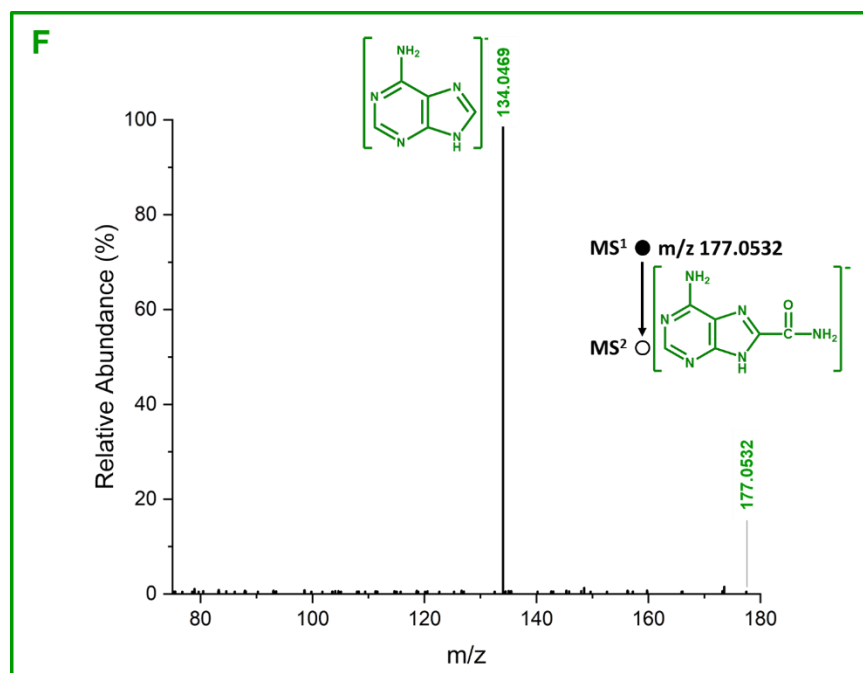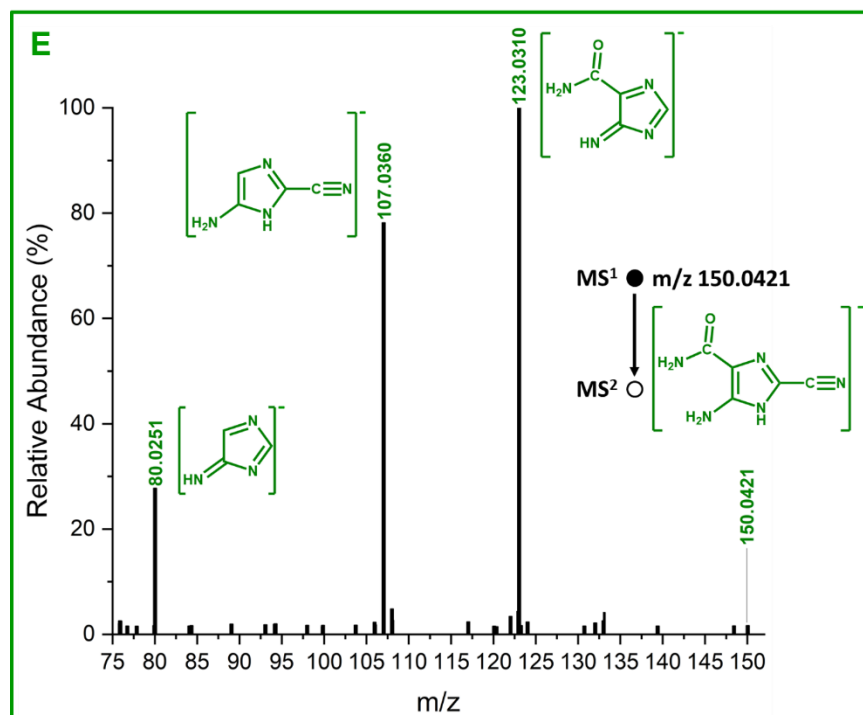
**Fig. S3.** Product ions ESI(-)-MS/MS spectra via CID for the precursor ions at m/z, 134 (A), 132 (B), 159 (C), 186 (D), 150 (E), and 177 (F). Possible structures of the deprotonated fragments are reported.

## References

1. M. Signorile, L. Zamirri, A. Tsuchiyama, P. Ugliengo, F. Bonino and G. Martra, *ACS Earth and Space Chem.*, 2020, **4**, 345-354.
2. G. Spoto, E. N. Gribov, G. Ricchiardi, A. Damin, D. Scarano, S. Bordiga, C. Lamberti and A. Zecchina, *Progress in Surface Science*, 2004, **76**, 71-146.
3. C. A. Cole, Z. C. Wang, T. P. Snow and V. M. Bierbaum, *J Phys Chem A*, 2015, **119**, 334-343.